Nuclear Inst. and Methods in Physics Research, A 1038 (2022) 166955

Contents lists available at ScienceDirect

Nuclear Inst. and Methods in Physics Research, A

journal homepage: www.elsevier.com/locate/nima

Evaluation of the DECAL Fully Depleted monolithic sensor for outer tracking and digital calorimetry

I. Kopsalis [a,*], P. Allport [a], S. Benhammadi [b], R. Bosley [a], J. Dopke [b], L. Fasselt [d], S. Flynn [a,1], P. Freeman [a,2], L. Gonella [a], N. Guerrini [b], C. Issever [c,d], K. Nikolopoulos [a], P. Phillips [b], T. Price [a], I. Sedgwick [b], E.G. Villani [a], M. Warren [e], N.K. Watson [a], H. Weber [d], F. Wilson [b], A. Winter [a], S. Worm [a,c], Z. Zhang [b]

[a] School of Physics and Astronomy, University of Birmingham, Edgbaston, B15 2TT, Birmingham, United Kingdom
[b] STFC Rutherford Appleton Laboratory, Harwell Campus, OX11 0QX, Didcot, United Kingdom
[c] Deutsches Elektronen-Synchrotron DESY, Platanenallee 6, D-15738, Zeuthen, Germany
[d] Institute for Physics, Humboldt University of Berlin, Newtonstrasse 15, D-12489, Berlin, Germany
[e] Department of Physics and Astronomy, University College London, Gower Street, WC1E 6BT, London, United Kingdom

ARTICLE INFO

Keywords:
Digital calorimetry
Depleted MAPS
TowerJazz modified process
Pixel equalisation matrix

ABSTRACT

The DECAL sensor is a depleted monolithic active pixel sensor (DMAPS) being developed to explore technological solutions for digital electromagnetic calorimeters. For this application, the number of pixels above threshold is used to estimate the shower energy and therefore the pixel size is required to be sufficiently small to avoid hit saturation. The DECAL and DECAL Fully Depleted (FD) sensors have been designed and fabricated in the TowerJazz 180 nm CMOS standard and modified imaging processes, respectively. The latter uses modifications to the implant configuration that improve charge collection and radiation hardness, including to the levels required for barrel ECAL regions of FCC-hh (few 10^{15} n_{eq}/cm^2). Both DECAL variants feature a matrix of 64 × 64 pixels with a pitch of 55 μm, read out every 25 ns. For DECAL FD, the logic has been modified to extend the in-pixel comparator threshold trim range from five to six bits, with the sixth bit used to de-activate the comparator. Characterisation results for the DECAL FD, including the pixel equalisation matrix, threshold scans testing under monochromatic X-rays and ^{90}Sr source, are presented.

1. Introduction

The primary aim of a Digital Electromagnetic Calorimeter is to count every particle that deposits energy above a given threshold within a high energy electromagnetic shower. This is intended to suppress the contribution from Landau fluctuations within the active material and improve the reconstruction of the incident particle energy. To avoid saturation arising from multiple particles hitting a single readout cell, very small cell sizes of order 50 μm are preferred. The feasibility and the advantages of using MAPS in the development of a highly granular DECAL are investigated in Refs. [1–3]. A DECAL sensor prototype [4,5] was designed by the team in Ref. [6] using the same process as for the 120 × 145 mm^2 3-side buttable 6.7 MPixel sensor. The long term project goal is the fabrication of a wafer scale DECAL sensor obtained by stitching. The prototype consists of 64 × 64 pixels of 55 μm pitch with total chip area 5 × 5 mm^2, and is read out using fast logic at 40 MHz. It provides the unique feature of being reconfigurable to function in two readout modes: a strip sensor, for particle tracking; or a pad sensor counting the number of pixels above threshold, for digital calorimetry. In strip mode, each strip corresponds to a 1 × 64 pixel column array and can record up to a maximum of three hits per column. In pad mode, each pad corresponds to a block of 16 × 64 pixel column arrays and can record up to a maximum of 15 hits per column, resulting in a maximum of 240 total counts per pad. Radiation hardness up to 10^{15} n_{eq}/cm^2 1 MeV neutron equivalent particle fluence has been demonstrated [7] in a novel variant of the same CMOS technology process with which the DECAL sensor is fabricated.

2. The DECAL fully depleted sensor

The DECAL FD is the second version of the DECAL sensor designed and fabricated in the TowerJazz 180 nm CMOS modified process on 25 μm epitaxial Si. The pixel design implements four collection electrodes placed in the pixel corners. The electronics are contained in a

* Corresponding author.
E-mail address: Ioannis.Kopsalis@stfc.ac.uk (I. Kopsalis).
[1] Current address: National Physical Laboratory, UK.
[2] Current address: University of California, Santa Barbara, CA, USA.

https://doi.org/10.1016/j.nima.2022.166955
Received 14 April 2022; Accepted 31 May 2022
Available online 8 June 2022

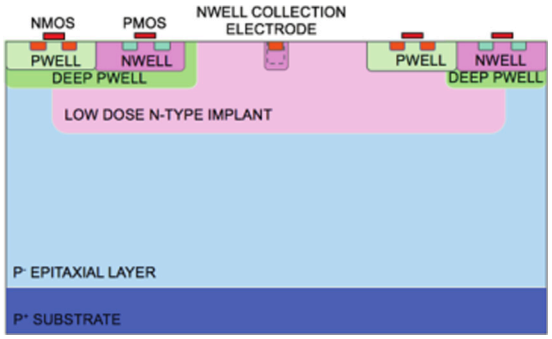

Fig. 1. Cross section of the modified TowerJazz 180 nm CMOS imaging process. The variant with an introduced gap in the n-layer near the pixel edge [8].

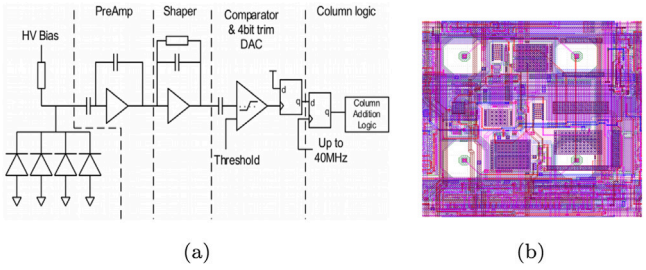

Fig. 2. (a) Pixel front-end architecture including the calibration DAC and comparator (b) GDS pixel design picture.

separate well outside the collection electrode. Depletion in the pixel area is achieved [8,9] by introducing a low dose, high energy n-type implant in the p-type epitaxial substrate, as shown in Fig. 1. With low reverse bias applied in both the p-well and the substrate, the p-type epitaxial layer is fully depleted from the n-well collection electrode to the highly doped p-type substrate. For the current prototype, full depletion is achieved by applying 0 V in the substrate and p-well, with +3.3 V in the n-well collection electrode. The improved charge collection performance of the above variant of the modified process is confirmed up to fluence levels of 10^{15} 1 MeV n_{eq}/cm^2 [10,11].

The DECAL FD sensor is similar to the previous design, with each pixel containing a common-source amplifier as a pre-amp, followed by a cascoded common-source amplifier configured as CR-RC shaper for noise reduction [12]. The diode is capacitively coupled, which allows high reverse voltage biasing through a large resistor, Fig. 2(a). The pre-amplifier input is biased through constant current feedback. Before reaching the comparator, the shaper output is passed through a capacitor whose bias is set by an in-pixel DAC. The DAC itself is a binary weighted current mirror where the current is applied through a 31 kΩ resistor. This voltage is then sampled in either polarity by a capacitor in the path of the signal from the shaper, allowing the threshold to be tuned to compensate for variations in the shaper DC level and comparator offset. With five bits, a granularity of the pixel trim up to 32 values is possible. The sixth bit is used as a pixel mask flag that de-activates the in-pixel comparator. The comparator determines whether input signals have crossed the detection threshold and is sampled by a global 40 MHz clock. The pixel design is implemented as shown in Fig. 2(b).

3. Pixel equalisation matrix

For all tests, the sensor is mounted on a custom designed PCB, Fig. 3, and read out with an Ethernet based system using the ATLAS ITSDAQ data acquisition software. The PCB allows all the bias voltages and currents to be controlled by software. It is vertically or horizontally mounted on the DECAL motherboard, which is connected to a Nexys

Fig. 3. The PCB with the mounted DECAL FD sensor.

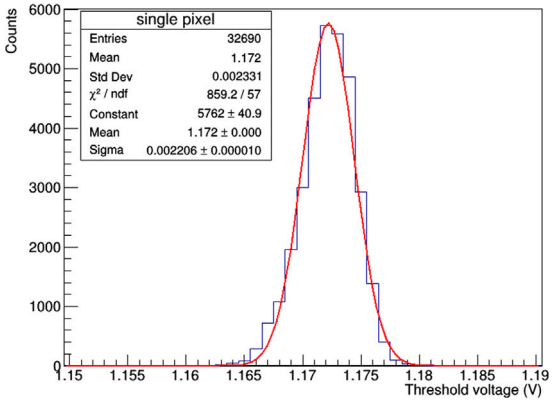

Fig. 4. Typical pixel threshold scan for a single pixel.

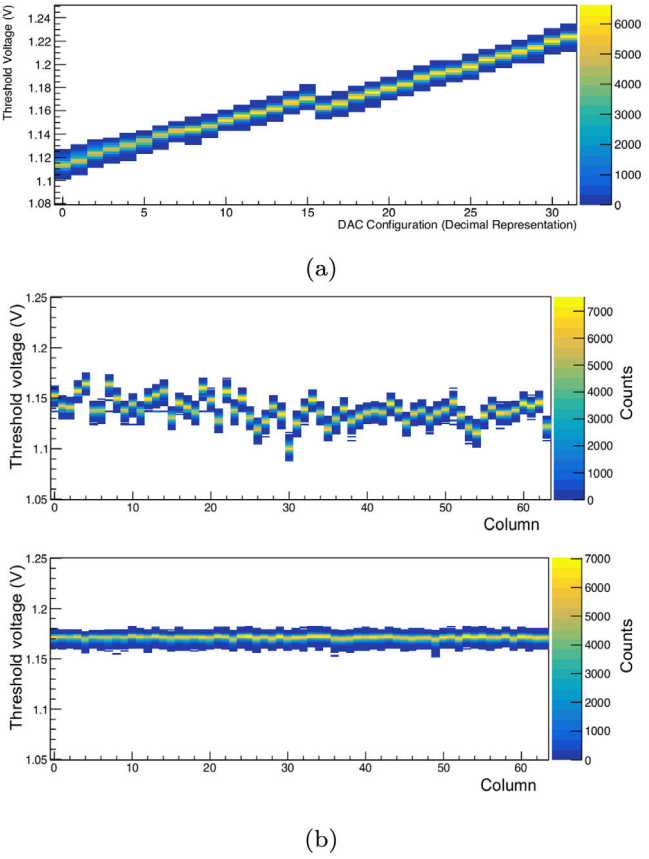

Fig. 5. (a) Threshold voltage as a function of pixel configuration and (b) Single pixel row before trimming (top) and after trimming (bottom) for all columns at threshold of 1.17 V.

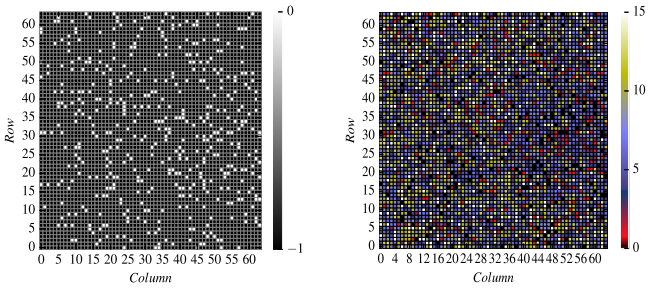

Fig. 6. (a) Polarity bit and (b) Pixel configuration of the 64 × 64 pixel matrix.

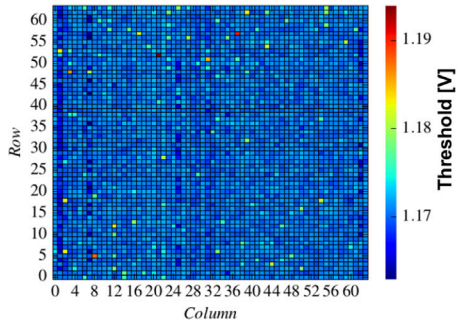

Fig. 7. Threshold voltage uniformity of the 64 × 64 pixel matrix.

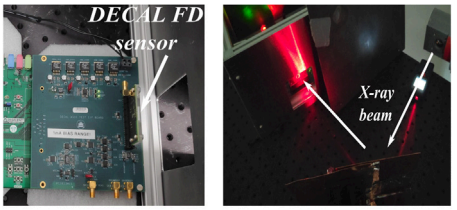

Fig. 8. (a) Photograph of the DECAL FD boards used to hold the PCB with the mounted sensor before and (b) during the X-ray illumination.

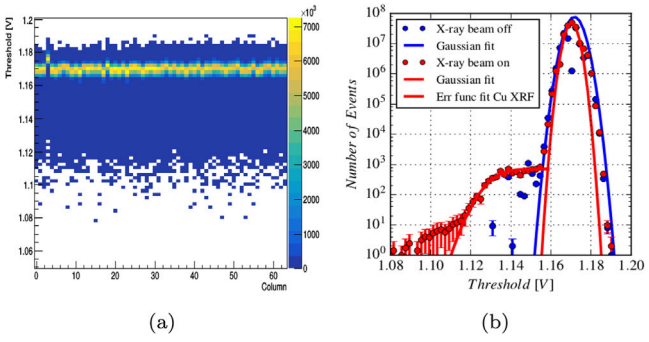

Fig. 9. (a) Threshold voltage as a function of pixel column for a single row during X-ray illumination and (b) Projection of the threshold voltage with X-ray beam off and on.

Video board through an FMC connector. Performing threshold scans in pixel columns and rows using trimming logic, the rate of hits in each pixel as a function of the applied threshold, allows the full chain from analogue to digital to be tested. Fig. 4 shows a single pixel threshold scan in absence of a physical signal, where the comparator does not fire if the input is far from the applied threshold. The mean threshold voltage is measured 1.172 V with $\sigma \approx 2$ mV. Tuning of the pixel matrix at uniform threshold voltage is achieved, performing threshold scans row by row. During the tuning process, the threshold voltage for every pixel is scanned to all possible configurations, Fig. 5(a). We observe a functional 4-bit DAC as well as polarity switching, where the latter introduces a slight offset. Fig. 5(b), presents the pixel threshold uniformity achieved for a single row before and after trimming. The mean threshold voltage is measured 1.170 V with $\sigma \approx 3$ mV. After completing the tuning process for 64 rows, the distribution of the polarity bits across the pixel matrix is presented in Fig. 6(a). The polarity is not reversed for the majority of the pixels. Fig. 6(b) presents the DAC configuration for every pixel in the matrix, varying between 0 and 15, after the completion of threshold tuning. The mean threshold voltage achieved for every pixel is presented in Fig. 7. Threshold uniformity within a 1 mV range is confirmed for more than 85% of all pixels in the 64 × 64 matrix. The ability to further improve the threshold uniformity is under development, investigating different tuning strategies. The sensor is operated at 0 V substrate voltage and +3.3 V in the n-well collection electrode at ambient room temperature 22 °C.

4. Performance tests with monochromatic X-rays and ^{90}Sr source

The conversion gain of the pixel front-end electronics is measured using an intense high-rate monochromatic X-ray source. Illuminating with X-rays from a tube, target material Cu, X-ray fluorescence photons are emitted with a characteristic K_α peak in the energy spectrum at E=8.05 keV. The main interaction process for this photon energy in Si is photoelectric absorption. The emitted electron generates electron–hole pairs. Electron–hole pair generation in Si requires energy $\epsilon \approx 3.6$ eV, so the generated signal is $E/\epsilon \approx 2236$ e$^-$. Fig. 8(a) shows the sensor vertically mounted and placed in front of an open window at a distance of 38 cm of 45° tilted Cu target. Photons from an industrial X-ray tube based at RAL, manufactured by Comet [13] and with W target material operated at 17 keV and 16 mA, illuminate the Cu target. Alignment is performed using a red laser pointer, Fig. 8(b). The energy spectrum of the Cu with the characteristic K_α peak is measured with the HEXITEC detector manufactured at RAL [14]. The measured photon rate at the sensor surface is 10^6 photons/s/cm^2.

Fig. 9 (a) presents a long-term threshold scan under X-ray illumination for a single pixel row after the threshold tuning process. Hits are recorded from all the pixel columns since the generated charge on the individual pixels causes shaper output voltage to drop. The plot shows a noise band at threshold values close to the shaper output remains level, along with a clear signal response from all the pixels. The threshold voltage range of the detected signal is ≈90 mV below the applied threshold, as presented in Fig. 9(b). Table 1 presents the Gaussian fitted parameters mean and σ with X-ray beam off and on, where no significant changes are observed.

The detected signal shape forms an Error function with a mean value of 1.13 V and $\sigma \approx 10$ mV. The absolute difference between the Gaussian

Table 1
Fit parameters to extract the conversion gain.

Fit functions	Mean [V]	σ [mV]
Beam off Gaussian	1.172	3
Beam on Gaussian	1.170	2
Beam on Err function	1.130	10

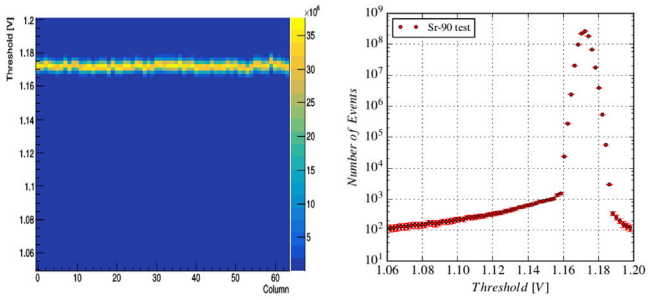

Fig. 10. (a) Threshold voltage as a function of pixel column for a single row and (b) Projection of the threshold voltage during ^{90}Sr irradiation.

and Error function mean ≈40 mV, is the measured signal amplitude. The conversion gain is calculated by dividing the signal amplitude with the generated signal 40 mV/2236 e^-≈18 μV/e^-.

The detection sensitivity of the sensor to minimum ionising particles (MIPs) is tested using a^{90}Sr radio-isotope of 160 MBq activity as a MIP source. Fig. 10(a) presents a long-term threshold scan using electrons emitted from the ^{90}Sr source for a single pixel row. Hits recorded from all the pixel columns with the threshold voltage range of the detected signal higher than 100 mV, are presented in Fig. 10(b). This non-realistic signal amplitude is related to the untriggered MIP signal recording. The synchronisation of the data recording time window and the information of a single MIP arrival time is under development. Improvements of the data acquisition firmware will resolve the above issue.

5. Conclusion

The DECAL FD sensor successfully demonstrates the digital functionality. The capability of six bits pixel trim range, where the sixth bit is used for pixel mask flag that de-activates the in-pixel comparator, improves substantially the pedestal and noise scans. Threshold uniformity within a 1 mV range is confirmed for pixels higher than 85% of total 64 × 64 pixel matrix. The conversion gain is extracted performing test with monochromatic X-rays. Although the data acquisition requires further improvements, evidence of MIP detection sensitivity is confirmed. Evaluation of the radiation hardness performance of the current prototype using the Birmingham proton irradiation facility is anticipated. A future larger area pixel matrix could be chosen as the candidate sensor for a test beam campaign of a composite SiW calorimeter.

Declaration of competing interest

The authors declare that they have no known competing financial interests or personal relationships that could have appeared to influence the work reported in this paper.

Acknowledgements

We thank Sion Richards and Matt Wilson for granting access and providing support to the X-ray tube facilities of the Technology Department at STFC-RAL. The authors gratefully acknowledge, the project funding received from the UK Research and Innovation - STFC Grant no. ST/N002911/1, the Birmingham Particle Physics Consolidated Grants: ST/N000463/1, ST/N001125/1, ST/P005888/1 and the European Union's Horizon 2020 Research and Innovation programme under Grant Agreement no. 654168.

References

[1] J.A. Ballin, et al., Monolithic active pixel sensors (MAPS) in a quadruple well technology for nearly 100% fill factor and full CMOS pixels, Sensors 8 (9) (2008) 5336, http://dx.doi.org/10.3390/s8095336.
[2] M. Aleksa, et al., Calorimeters for the FCC-hh, CERN-FCC-PHYS-2019-0003, https://cds.cern.ch/record/2705432/files/1912.09962.pdf.
[3] The ALICE Collaboration, Letter of Intent: A forward calorimeter (FoCal) in the ALICE experiment, https://cds.cern.ch/record/2719928/files/LHCC-I-036.pdf.
[4] P.P. Allport, et al., First tests of a reconfigurable depleted MAPS sensor for digital electromagnetic calorimetry, Nucl. Inst. Meth. A 958 (2020) 162654, http://dx.doi.org/10.1016/j.nima.2019.162654.
[5] P. Allport, et al., A reconfigurable CMOS sensor for tracking, pre-shower and digital electromagnetic calorimetry, Nucl. Inst. Meth. A 978 (2020) 164459, http://dx.doi.org/10.1016/j.nima.2020.164459.
[6] I. Sedgwick, et al., LASSENA: A 6.7 megapixel, 3-sides buttable wafer-scale CMOS sensor using a novel grid-addressing architecture, 2013, International Image Sensor Society, https://imagesensors.org/2013-papers.
[7] M. Dyndal, et al., Mini-MALTA: radiation hard pixel designs for small-electrode monolithic CMOS sensors for the high luminosity LHC, J. Instrum. 15 (2020) P02005, http://dx.doi.org/10.1088/1748-0221/15/02/P02005.
[8] W. Snoeys, Development of monolithic sensors for high energy physics in commercial CMOS technologies, Nucl. Inst. Meth. A 938 (2019) 41–50, http://dx.doi.org/10.1016/j.nima.2019.05.033.
[9] W. Snoeys, et al., A process modification for CMOS monolithic active pixel sensors for enhanced depletion, timing performance and radiation tolerance, Nucl. Inst. Meth. A 871 (2017) 90–96, http://dx.doi.org/10.1016/j.nima.2017.07.046.
[10] H. Pernegger, Depleted CMOS sensors for HL-LHC, Proc. Sci. 348 (2022) http://dx.doi.org/10.22323/1.348.0041, (VERTEX2018).
[11] M. Munker, et al., Simulations of CMOS pixel sensors with a small collection electrode, improved for a faster charge collection and increased radiation tolerance, J. Instrum. 14 (2019) C05013, http://dx.doi.org/10.1088/1748-0221/14/05/C05013.
[12] S. Benhammadi, DECAL: A reconfigurable monolithic active pixel sensor for use in calorimetry and tracking, Proc. Sci. 370 (2022) http://dx.doi.org/10.22323/1.370.0040, (TWEPP2019).
[13] Comet X-ray tubes, https://www.comet-xray.cn/zh/products/x-ray-tubes/tubes/mxr-160-3.
[14] Quantum detectors Ltd, RAL, Harwell, OX11 0QX, UK, high energy X-ray imaging technology detector, https://quantumdetectors.com/products/hexitec/.